

# Constrained Nonlinear Tracking Control for Small Fixed-wing Unmanned Air Vehicles

Wei Ren and Randal W. Beard

**Abstract**— This paper considers the problem of constrained nonlinear tracking control for small fixed-wing unmanned air vehicles equipped with longitudinal and lateral autopilots. Four different controllers based on SDRE, Sontag’s formula, geometric mean, and aggressive selection from the feasible control set are proposed and compared to show their strengths and weaknesses under different application scenarios. Issues of measurement noise and input uncertainties are also addressed under the input-to-state stability framework. The effectiveness of the approaches is demonstrated through detailed simulation studies.

## I. INTRODUCTION

Controller design for systems subject to input constraints offers both practical significance and theoretical challenges to the control community. Two effective approaches for the design of nonlinear controllers are control Lyapunov functions (CLFs) [1], [2] and receding horizon control (RHC)/model predictive control (MPC), [3]. Both approaches can be extended to find control laws for nonlinear systems subject to certain input constraints. In [4] and [5], constrained CLFs are applied to construct stabilizing universal formulas respectively for systems with control inputs bounded in a Euclidean norm sense and systems with a scalar control input that is positive and/or bounded. Input constraints can also be incorporated into the MPC framework, which is known as the constrained MPC (c.f. [3]). The issues limiting the RHC approach are its computation requirements and stability concerns.

In this paper, we consider the problem of constrained nonlinear tracking control for small fixed-wing unmanned air vehicles (UAVs). The inherent properties of fixed-wing UAVs impose the input constraints of positive minimum velocity, bounded maximum velocity, and saturated heading rate. Equipping a UAV with standard longitudinal and lateral autopilots, its dynamics can be modelled by kinematic equations of motion that are similar to those of nonholonomic mobile robots.

In [6], a constrained tracking CLF is constructed and a simple saturation controller based on this CLF is proposed for the UAV tracking control problem, where issues like input uncertainties and measurement noise are not considered. In this paper, we extend the results in [6] by proposing four different tracking controllers and comparing them with each other to show relative strengths and weaknesses under different situations. The first approach is based on the state dependent Riccati equation (SDRE) methodology [7]. The second approach is based on Sontag’s formula. The third approach uses a CLF and chooses the geometric center of the feasible input set. The last approach follows the

saturation controller in [6] but explicitly accounts for input uncertainties under the input-to-state (ISS) framework [8]. Although these approaches are designed specifically for UAVs, the design strategy can be applied to general systems. That is, if a constrained CLF can be found for a system with input constraints, the feasible control set that defines all the stabilizing controls with respect to the CLF satisfying the input constraints can be specified accordingly (see [9] for a complete parametrization of the unconstrained stabilizing controls with respect to a certain CLF). Then unconstrained controllers based on existing approaches (e.g. universal formulas, min-norm solutions, backstepping, sliding mode, SDRE, LQR) can be projected pointwise onto the feasible control set in a certain way (e.g. find the closest element in the set). The resulting control laws not only guarantee stability but also satisfy the input constraints. In addition, direct parametrization of the feasible set, e.g. our third approach, can also be applied. Of course, the above design methodology requires finding a constrained CLF, which may be challenging for general nonlinear systems.

## II. PROBLEM STATEMENT

The overall system architecture considered in this paper consists of five layers [10]: Waypoint Path Planner (WPP), Dynamic Trajectory Smoother (DTS), Trajectory Tracker (TT), Longitudinal and Lateral Autopilots, and the UAV as shown in Figure 1.

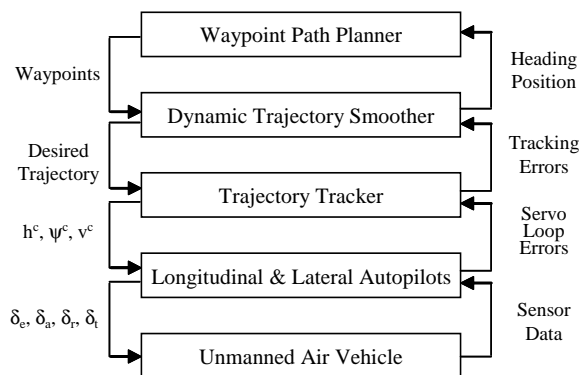


Fig. 1. System Architecture.

The WPP generates waypoint paths (straight-line segments) that change in accordance with the dynamic environment consisting of the location of the UAV, the targets, and the dynamically changing threats. The DTS smoothes through these waypoints and produces a feasible time-parameterized desired trajectory, that is, the desired position  $(x_r(t), y_r(t))$ , heading  $\psi_r(t)$ , and altitude  $h_r(t)$ . The TT outputs the velocity command  $v^c$ , heading command  $\psi^c$ , and altitude command  $h^c$  to the autopilots based on the

This work was funded by AFOSR grants F49620-01-1-0091 and F49620-02-C-0094, and by DARPA grant NBCH1020013.

W. Ren and R. W. Beard are with the Department of Electrical and Computer Engineering, Brigham Young University, Provo, Utah 84602, USA {weiren, beard}@ee.byu.edu

desired trajectory. The autopilots then use these commands to control the elevator,  $\delta_e$ , aileron,  $\delta_a$ , rudder  $\delta_r$ , and throttle  $\delta_t$ , of the UAV [10]. In this paper we focus on the trajectory tracker.

With the UAV equipped with standard autopilots, the resulting UAV/autopilot models are assumed to be first order for heading and Mach hold, and second order for altitude hold [11]. Letting  $(x, y)$ ,  $\psi$ ,  $v$ , and  $h$  denote the inertial position, heading angle, velocity, and altitude of the UAV respectively, the kinematic equations of motion are given by

$$\begin{aligned}\dot{x} &= v \cos(\psi) \\ \dot{y} &= v \sin(\psi) \\ \dot{\psi} &= \alpha_\psi(\psi^c - \psi) \\ \dot{v} &= \alpha_v(v^c - v), \\ \dot{h} &= -\alpha_h \dot{h} + \alpha_h(h^c - h),\end{aligned}\quad (1)$$

where  $\psi^c$ ,  $v^c$ , and  $h^c$  are the commanded heading angle, velocity, and altitude to the autopilots, and  $\alpha_*$  are positive constants [11].

In the remainder of the paper, we assume that the altitude controller follows the design presented in [12], and focus on the design of the velocity and heading controller. We assume that the velocity-heading dynamics are adequately modelled by

$$\begin{aligned}\dot{x} &= v^c \cos(\psi) \\ \dot{y} &= v^c \sin(\psi) \\ \dot{\psi} &= \omega^c,\end{aligned}\quad (2)$$

where  $\omega^c = \alpha_\psi(\psi^c - \psi)$  [6]. The dynamics of the UAV impose the following input constraints

$$\mathcal{U}_1 = \{v^c, \omega^c | 0 < v_{min} \leq v^c \leq v_{max}, \\ -\omega_{max} \leq \omega^c \leq \omega_{max}\}.\quad (3)$$

The desired trajectory  $(x_r, y_r, \psi_r, v_r, \omega_r)$  generated by the trajectory generator also satisfies Eq. (2) in structure under the constraints that  $v_r$  and  $\omega_r$  are piecewise continuous and satisfy the constraints

$$\begin{aligned}v_{min} + \epsilon_v \leq v_r \leq v_{max} - \epsilon_v \\ -\omega_{max} + \epsilon_\omega \leq \omega_r \leq \omega_{max} - \epsilon_\omega,\end{aligned}\quad (4)$$

where  $\epsilon_v$  and  $\epsilon_\omega$  are positive control parameters.

By transforming the tracking errors expressed in the inertial frame as  $(x_r - x, y_r - y, \psi_r - \psi)$  into the UAV body frame denoted as  $(x_e, y_e, \psi_e)$  and introducing the change of variables [13]

$$(x_0, x_1, x_2) \triangleq (\psi_e, y_e, -x_e) \quad (5)$$

and  $u_0 \triangleq \omega_r - \omega^c$  and  $u_1 \triangleq v^c - v_r \cos(x_0)$ , we obtain

$$\begin{aligned}\dot{x}_0 &= u_0 \\ \dot{x}_1 &= (\omega_r - u_0)x_2 + v_r \sin(x_0) \\ \dot{x}_2 &= -(\omega_r - u_0)x_1 + u_1.\end{aligned}\quad (6)$$

The input constraints under the transformation become

$$\mathcal{U}_2 = \{u_0, u_1 | \underline{\omega} \leq u_0 \leq \bar{\omega}, \underline{v} \leq u_1 \leq \bar{v}\}, \quad (7)$$

where  $\underline{v} \triangleq v_{min} - v_r \cos(x_0)$ ,  $\bar{v} \triangleq v_{max} - v_r \cos(x_0)$ ,  $\underline{\omega} \triangleq \omega_r - \omega_{max}$ , and  $\bar{\omega} \triangleq \omega_r + \omega_{max}$  are time-varying.

Note from Eq. (6) that  $x_1$  is not directly controlled by  $u_0$  and  $u_1$ . To avoid this situation we introduce another change of variables.

Let  $\bar{x}_0 \triangleq mx_0 + \frac{x_1}{\pi_1}$ , where  $m > 0$  and  $\pi_1 \triangleq \sqrt{x_1^2 + x_2^2 + 1}$ . Accordingly,  $x_0 \triangleq \frac{\bar{x}_0}{m} - \frac{x_1}{m\pi_1}$ . Obviously,  $(\bar{x}_0, x_1, x_2) = (0, 0, 0)$  is equivalent to  $(x_0, x_1, x_2) = (0, 0, 0)$  and  $(x_e, y_e, \psi_e) = (0, 0, 0)$ . The original tracking control objective, that is, find  $v^c$  and  $\omega^c$  such that  $|x_r - x| + |y_r - y| + |\psi_r - \psi| \rightarrow 0$  as  $t \rightarrow \infty$ , is converted to a stabilization objective, that is, find control inputs  $u_0$  and  $u_1$  to stabilize  $(\bar{x}_0, x_1, x_2)$ . With the same input constraints (7), Eq. (6) can be rewritten as

$$\dot{x} = f_1(t, x) + g_1(x)[u_0, u_1]^T, \quad (8)$$

where  $x = [\bar{x}_0, x_1, x_2]^T$ ,

$$f_1(t, x) = \begin{bmatrix} \frac{x_2}{\pi_1} \omega_r + \frac{1+x_2^2}{\pi_1^3} v_r \sin\left(\frac{\bar{x}_0}{m} - \frac{x_1}{m\pi_1}\right) \\ x_2 \omega_r + v_r \sin\left(\frac{\bar{x}_0}{m} - \frac{x_1}{m\pi_1}\right) \\ -\omega_r x_1 \end{bmatrix}$$

and

$$g_1(x) = \begin{bmatrix} m - \frac{x_2}{\pi_1} & -\frac{x_1 x_2}{\pi_1^3} \\ -x_2 & 0 \\ x_1 & 1 \end{bmatrix}.$$

Define

$$\begin{aligned}W(x) &= \gamma_0 \left(\frac{\bar{x}_0}{\pi_2}\right)^2 + \gamma_1 k_1 (v_{min} + \epsilon_v) \frac{x_1}{\pi_1} \sin\left(\frac{x_1}{m\pi_1}\right) \\ &+ \gamma_2 \left(k_1 - \frac{1}{2}\right) \left(\frac{x_2}{\pi_1}\right)^2 \left[ (v_{min} + \epsilon_v) \cos\left(\frac{x_1}{m\pi_1}\right) - v_{min} \right],\end{aligned}\quad (9)$$

where  $\pi_2 \triangleq \sqrt{\bar{x}_0^2 + 1}$ ,  $k_1 > \frac{1}{2}$ ,  $\gamma_0 > 0$ , and  $0 < \gamma_1, \gamma_2 < 1$ .

It has been shown in [6] that for  $m > \kappa$ , where  $\kappa$  is a positive constant made precise in [6],

$$V(x) = \sqrt{\bar{x}_0^2 + 1} + k_1 \sqrt{x_1^2 + x_2^2 + 1} - (1 + k_1) \quad (10)$$

is a constrained CLF for system (8) with input constraints (7) such that  $\inf_{u \in \mathcal{U}_2} \dot{V} \leq -W(x)$ , where  $W(x)$  is a continuous positive-definite function given by Eq. (9).

### III. NONLINEAR TRACKING CONTROL FOR UAVS

In this section, we propose two nonlinear tracking controllers for UAVs. They have the property that input constraints are not explicitly considered. The first controller is derived using the SDRE approach and the second is based on Sontag's formula.

#### A. SDRE Tracking Controller

The SDRE nonlinear regulator is derived to minimize the performance index  $J = \frac{1}{2} \int_0^\infty x^T Q(x)x + u^T R(x)u dt$  for the affine nonlinear system

$$\dot{x} = f(x) + g(x)u, \quad (11)$$

where  $x \in \mathbb{R}^n$ ,  $u \in \mathbb{R}^m$ ,  $Q(x) > 0$ ,  $R(x) > 0$ ,  $\forall x$ ,  $f(x) \in C^1$ , and  $f(0) = 0$ .

Motivated by the LQR approach for LTI systems, Eq. (11) can be represented as

$$\dot{x} = A(x)x + B(x)u, \quad (12)$$

where  $A(x)x = f(x)$  and  $B(x) = g(x)$ .

Under the condition that the pair  $(A(x), B(x))$  is pointwise stabilizable, the nonlinear state feedback control law can be constructed as

$$u_{SDRE} = -R^{-1}(x)B^T(x)P(x)x, \quad (13)$$

where  $P(x) > 0$  is obtained by solving the state-dependent Riccati equation  $A^T P + PA - PBR^{-1}B^T P + Q = 0$  pointwise at each state  $x$ .

It has been shown that the SDRE regulator is locally asymptotically stable and suboptimal [7].

System (6) can be written as  $\dot{x} = A(t, x)x + B(x)u$ , where  $x = [x_0, x_1, x_2]^T$ ,  $u = [u_0, u_1]^T$ ,

$$A(t, x) = \begin{bmatrix} 0 & 0 & 0 \\ v_r(t) \frac{\sin(x_0)}{x_0} & 0 & \omega_r(t) \\ 0 & -\omega_r(t) & 0 \end{bmatrix}$$

and

$$B(x) = \begin{bmatrix} 1 & 0 \\ -x_2 & 0 \\ x_1 & 1 \end{bmatrix}.$$

The pointwise controllability matrix is given by  $C(t, x) = [B(x), A(t, x)B(x), A(t, x)^2 B(x)]$ . It can be verified that  $C(t, x)$  has full rank when  $\omega_r(t) \neq 0$ . When  $\omega_r(t) = 0$  at some time  $t = t^*$ , it can be seen that  $C(t, x)$  still has full rank if and only if  $x_0 \neq k\pi$ ,  $k \in \mathbf{Z} \setminus 0$ . As a result,  $(A(t, x), B(x))$  is pointwise stabilizable as long as  $x_0 \neq k\pi$ ,  $k \in \mathbf{Z} \setminus 0$ .

Note that unlike the standard SDRE regulation problem, matrix  $A(t, x)$  factorized from Eq. (11) is also an explicit function of time since the reference velocity  $v_r(t)$  and reference heading rate  $\omega_r(t)$  are time-varying. The SDRE tracking controller will be obtained by following Eq. (13) except that the pointwise solution to the SDRE, denoted as  $P(t, x)$ , is also an explicit function of time in this case. This results from the fact that the state is regulated to a time-varying trajectory instead of a constant reference state. Also note that the SDRE controller is designed according to the original system (6) rather than system (8) with the change of variables introduced. Of course, it is also valid to design the SDRE controller according to system (8). However, the SDRE design based on the original system (6) may be superior to the SDRE design based on system (8) under some situations since the change of variables introduces extra weightings.

Define a saturation function as

$$\text{sat}(\alpha, \beta, \gamma) = \begin{cases} \beta, & \alpha < \beta \\ \alpha, & \beta \leq \alpha \leq \gamma \\ \gamma, & \alpha > \gamma \end{cases}$$

where it is assumed that  $\beta < \gamma$ . Note that the control  $u_{SDRE} = [u_a, u_b]^T$  may not satisfy the input constraints (7). The actual control will be saturated to satisfy (7) according to a simple projection as follows:

$$\begin{aligned} u_0 &= \text{sat}(u_a, \underline{u}, \bar{u}) \\ u_1 &= \text{sat}(u_b, \underline{v}, \bar{v}). \end{aligned} \quad (14)$$

## B. Tracking Controller Based on Sontag's Formula

For system (11), a globally asymptotically stabilizing control law known as Sontag's formula [14], [15] is given by

$$u_s = \begin{cases} -\frac{L_f V + \sqrt{(L_f V)^2 + (L_g V (L_g V)^T)^2}}{L_g V (L_g V)^T} (L_g V)^T, & L_g V \neq 0 \\ 0, & L_g V = 0 \end{cases} \quad (15)$$

where  $V(x)$  is a CLF for system (11).

The tracking controller for UAVs based on Sontag's formula can be defined following Eq. (15) with  $L_f V = \frac{\partial V}{\partial x} f_1(t, x)$  and  $L_g V = \frac{\partial V}{\partial x} g_1(x)$ , where  $V(x)$  is the constrained CLF given by (10). Note that although the universal formula (15) is originally proposed for time-invariant systems, the formula is also valid for the time-varying system (8) due to the fact that the CLF for system (8) is not an explicit function of time. However, there is no guarantee that the control  $u_s(t, x)$  given by Eq. (15) will satisfy the input constraints (7) since Sontag's formula is based on the assumption that  $u \in \mathbb{R}^m$ . Similar to the SDRE controller, the actual control is a projection of  $u_s(t, x) = [u_c, u_d]$  to the space defined by the input constraints (7) as follows

$$\begin{aligned} u_0 &= \text{sat}(u_c, \underline{u}, \bar{u}) \\ u_1 &= \text{sat}(u_d, \underline{v}, \bar{v}). \end{aligned} \quad (16)$$

## IV. CONSTRAINED NONLINEAR TRACKING CONTROL FOR UAVS

In this section, we introduce two other nonlinear tracking controllers which explicitly account for input constraints.

### A. Tracking Controller Based on the Geometric Center of the Feasible Set

Define the feasible control set as

$$\mathcal{F}(t, x) = \{u \in \mathcal{U}_2 | L_{f_1} V + L_{g_1} V u \leq -W(x)\},$$

where  $W(x)$  is given by Eq. (9). Note that the fact that  $V$  is a constrained CLF for system (8) guarantees that  $\mathcal{F}(t, x)$  is nonempty for any  $t$  and  $x$ .

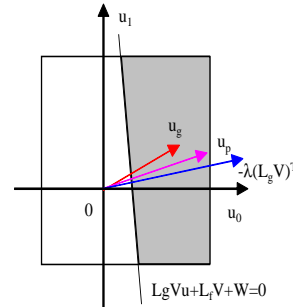


Fig. 2. The feasible set  $\mathcal{F}(t, x)$  at time  $t = t_1$ .

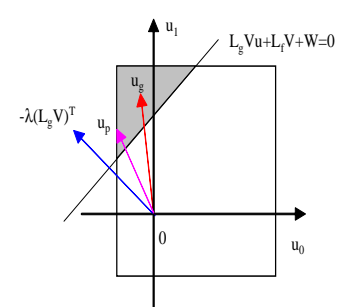


Fig. 3. The feasible set  $\mathcal{F}(t, x)$  at time  $t = t_2$ .

Fig. 2 and 3 show the feasible set at time  $t = t_1$  and  $t = t_2$  respectively. The line denoted by  $L_{g_1} V u + L_{f_1} V + W = 0$  separates the 2-D control space into two halves, where the right half in Fig. 2 and the left half in Fig. 3 represent the unconstrained stabilizing controls satisfying  $\dot{V} \leq -W(x)$  at time  $t_1$  and  $t_2$  respectively. The rectangle area denotes

the time-varying input constraints (7). The shaded area represents the stabilizing controls which also satisfy input constraints (7), that is, the feasible set  $\mathcal{F}(t, x)$ . In Fig. 2 and 3,  $u_g$  represents the geometric center of the feasible set. Obviously, such controls will stay in the feasible set at each time.

As a comparison, we also plot the vector  $-\lambda(L_{g_1}V)^T$  in both figures, where  $\lambda > 0$ . Note that this vector is orthogonal to the line  $L_{g_1}Vu + L_{f_1}V + W = 0$ . It can be verified that the control based on Sontag's formula in Section III-B can be represented as  $u_s(t, x) = -\chi(t, x)(L_{g_1}V)^T$ , where  $\chi(t, x)$  is a nonnegative scalar function of  $t$  and  $x$ . Therefore, the control based on Sontag's formula lies along the vector  $-\lambda(L_{g_1}V)^T$  but may have a different magnitude. In Fig. 2, we can see that the control based on Sontag's formula may or may not stay in the feasible set depending on its magnitude. However, a proper scale of the control can always bring it back to the feasible set. With the input constraints (7), the actual control will be a projection of  $u_s(t, x)$  to the rectangle region. As shown in Fig. 2, a projection of  $u_s(t, x)$ , denoted as  $u_p$ , is either inside the feasible set or on the boundary of the feasible set depending on its magnitude. In either case, the projected control based on Sontag's formula guarantees stability even if there are input constraints. In Fig. 3, we can see that the control based on Sontag's formula cannot stay within the feasible set even with some scaling due to its direction. In this case, a projection of  $u_s(t, x)$  is not guaranteed to stay within the feasible set. However, it is straightforward to see that  $\nu u_s(t, x)$ , where  $\nu > 1$ , is still a stabilizing control in the case of  $u \in \mathbb{R}^m$ . As a result, for a stabilizing control  $\nu u_s(t, x)$  with significantly large magnitude, the projection of  $\nu u_s(t, x)$  to the rectangle area, denoted as  $u_p$ , is guaranteed to be on the boundary of the feasible set as shown in Fig. 3, which in turn guarantees stability. Note that the projection of the SDRE control (14) to the rectangle area is not guaranteed to be within the feasible set since the SDRE control may not guarantee global stability even in the case of unconstrained control inputs. That is, the SDRE control may not even point toward the unconstrained stabilizing area. Of course, this disadvantage can be corrected by projecting the SDRE control to the feasible set rather than the entire constrained input space at each time. In this paper, we still project the SDRE control to the entire constrained input space as given by Eq. (14) for comparison purposes.

### B. Saturation Tracking Controller Generated from the Feasible Set

Consider the following affine nonlinear time-varying system with control input  $u$  and disturbance  $d$

$$\dot{x} = f(t, x) + g(t, x)u + g_d(t, x)d, \quad (17)$$

where  $x \in \mathbb{R}^n$ ,  $u \in \mathbb{R}^m$ ,  $d \in \mathbb{R}^r$ , and  $f : \mathbb{R}_+ \times \mathbb{R}^n \rightarrow \mathbb{R}^n$ ,  $g : \mathbb{R}_+ \times \mathbb{R}^n \rightarrow \mathbb{R}^{n \times m}$ , and  $g_d : \mathbb{R}_+ \times \mathbb{R}^n \rightarrow \mathbb{R}^{n \times r}$  are locally Lipschitz in  $x$  and piecewise continuous in  $t$ . In Eq. (17), the term  $g_d(t, x)d$  represents the perturbation to the original system  $\dot{x} = f(t, x) + g(t, x)u$ , which may result from model uncertainties, disturbances, and so on [15].

We have the following definition for an input-to-state stabilizing control Lyapunov function (ISS-CLF) (see [15]).

*Definition 1:* A continuously differentiable function  $V : \mathbb{R}_+ \times \mathbb{R}^n \rightarrow \mathbb{R}$  is an ISS-CLF for system (17) if it is positive-definite, decrescent, radially unbounded in  $x$  and there exist class  $\mathcal{K}$  functions  $\alpha(\cdot)$  and  $\rho(\cdot)$  such that

$$\inf_{u \in \mathbb{R}^m} L_f V + L_g V u + L_{g_d} V d + \frac{\partial V}{\partial t} \leq -\alpha(\|x\|), \quad \forall \|x\| \geq \rho(\|d\|).$$

Given  $W(x)$  in Eq. (9), there exists a class  $\mathcal{K}$  function  $\chi_w$  such that  $\chi_w(\|x\|) \leq W(x)$ ,  $\forall x$  ([16], Lemma 3.5).

*Lemma 2:* Let  $\mu = \sup_{\|x\| \rightarrow \infty} \chi_w(\|x\|)$  and  $b_1 = [1, k_1, k_1]^T$ . If  $\|d\| < \frac{\lambda\mu}{\|b_1\|}$ , where  $0 < \lambda < 1$ , then  $V(x)$  is also an ISS-CLF with input constraints (7) for system

$$\dot{x} = f_1(t, x) + g_1(x)u + d, \quad (18)$$

where  $d$  is the perturbation term to the nominal system (8).

*Proof:* Note that  $\frac{\partial V}{\partial x} = [\frac{\bar{x}_0}{\pi_2}, k_1 \frac{x_1}{\pi_1}, k_1 \frac{x_2}{\pi_1}]$ , where  $|\frac{\bar{x}_0}{\pi_2}| < 1$ ,  $|\frac{x_1}{\pi_1}| < 1$ , and  $|\frac{x_2}{\pi_1}| < 1$ .

It can be seen that

$$\begin{aligned} & \inf_{u \in \mathcal{U}_2} \frac{\partial V}{\partial x} f_1 + \frac{\partial V}{\partial x} g_1 u + \frac{\partial V}{\partial x} d \\ & \leq -W(x) + \left\| \frac{\partial V}{\partial x} d \right\| \\ & \leq -(1 - \lambda)\chi_w(\|x\|) - \lambda\alpha_w(\|x\|) + \|b_1\| \|d\| \\ & \leq -(1 - \lambda)\chi_w(\|x\|), \quad \forall \|x\| \geq \alpha_w^{-1} \left( \frac{\|b_1\| \|d\|}{\lambda} \right) \end{aligned}$$

Note that  $\alpha_w^{-1}(\cdot)$  in the last inequality is also a class  $\mathcal{K}$  function of  $\|d\|$  and is well defined since  $\frac{\|b_1\| \|d\|}{\lambda} < \mu$ . ■

Note that here  $\chi_w(\cdot)$  is a class  $\mathcal{K}$  function instead of a class  $\mathcal{K}_\infty$  function, which in turn imposes constraints for  $\|d\|$ . This can be explained from the constrained input perspective. In the case of  $d = 0$ , the derivative of the CLF cannot approach  $-\infty$  as the tracking errors approach  $\infty$  even with maximum control authority due to the saturated controls. As a result,  $\chi_w(\cdot)$  can only be a class  $\mathcal{K}$  function given the input constraints.

Let

$$u_0 = \text{sat}(-\eta_\omega \bar{x}_0, \underline{\omega}, \bar{\omega}) \quad (19)$$

$$u_1 = \text{sat}(-\eta_v x_2, \underline{v}, \bar{v}). \quad (20)$$

It has been shown in [17] that the above control law aggressively selected from the feasible set globally asymptotically stabilizes system (8) with input constraints (7) for sufficiently large  $\eta_v > 0$  and  $\eta_\omega > 0$  made precise in [17].

Note that the commanded velocity and heading rate to the autopilots are defined as  $v^c \triangleq u_1 + v_r \cos(x_0)$  and  $\omega^c \triangleq \omega_r - u_0$ . It is obvious that the commanded control  $v^c$  and  $\omega^c$  rely on the state measurement  $x$ ,  $y$ , and  $\psi$ . Due to measurement noise, there exist input uncertainties for  $[v^c, \omega^c]^T$ . Equivalently, we may consider input uncertainties for  $[u_0, u_1]^T$  in system (8). We denote the actual control input to system (8) as  $u = [u_0 + \Delta u_0, u_1 + \Delta u_1]^T$ , where  $\Delta u_0$  and  $\Delta u_1$  represent the uncertainties. Due to saturation constraints, we know that  $|\Delta u_0| \leq 2\omega_{max}$  and  $|\Delta u_1| \leq v_{max} - v_{min}$ .

We have the following lemma considering input uncertainties.

*Lemma 3:* Let  $b_2 = [m + 1, k_1 + \frac{1}{2}]^T$  and  $\Delta u = [\Delta u_0, \Delta u_1]^T$ . If  $\|\Delta u\| < \frac{\lambda \mu}{\|b_2\|}$ , where  $0 < \lambda < 1$ , then  $V(x)$  is an ISS-Lyapunov function for system (8) with control inputs given by Eqs. (19) and (20) and  $d = g_1 \Delta u$ .

*Proof:* Noting that

$$\frac{\partial V}{\partial x} g_1 = \left[ \left( m - \frac{x_2}{\pi_1} \right) \frac{\bar{x}_0}{\pi_2}, -\frac{\bar{x}_0}{\pi_2} \frac{x_1 x_2}{\pi_1^3} + k_1 \frac{x_2}{\pi_1} \right],$$

where  $\left| \left( m - \frac{x_2}{\pi_1} \right) \frac{\bar{x}_0}{\pi_2} \right| < m + 1$ , and  $\left| -\frac{\bar{x}_0}{\pi_2} \frac{x_1 x_2}{\pi_1^3} + k_1 \frac{x_2}{\pi_1} \right| < k_1 + \frac{1}{2}$ , the result then directly follows Lemma 2. ■

## V. SIMULATION RESULTS

In this section, we simulate several scenarios where the four tracking controllers proposed in Section III and IV are applied to a small fixed-wing UAV to track a time-parameterized desired trajectory that satisfies the constraints (4).

The parameters used in the simulation are chosen as  $\alpha_\psi = 5$ ,  $\alpha_v = 50$ ,  $\epsilon_v = 0.2$  (m/s),  $\epsilon_\omega = 0.2$  (rad/s),  $k_1 = 2$ ,  $\gamma_0 = \gamma_1 = \gamma_2 = 0.5$ ,  $\eta_\omega = \eta_v = 10$ , and  $m = 1$ . Note that the value for  $m$  is much lower than the theoretical lower bound defined in [6]. However, as we will see in the following, the controllers work well using this value, which implies the robustness of the controllers to parameter variations. We assume arbitrarily that the commanded velocity and heading rate are saturated at  $v^c \in [1.0, 1.8]$  (m/s) and  $|\omega^c| \leq 1.5$  (rad/s) to test the performance of the controllers.

Fig. 4 shows the desired trajectory generated from the DTS and the actual trajectories generated from the four tracking controllers under small initial errors. For the SDRE controller, the weighting matrices are chosen as  $Q(x) = \text{diag}([1, 1, 1])$  and  $R(x) = \frac{100}{(\sqrt{x_0^2 + x_1^2 + x_2^2} + 0.2)} \text{diag}([1, 1])$ . Fig. 5 shows the distance and heading tracking errors and Fig. 6 shows the desired and actual control inputs under the same initial conditions. We can see that all four controllers guarantee asymptotic tracking. Although the controller based on Sontag's formula does not explicitly consider the input constraints, the tracking errors using the projection of that controller converge fastest. On the other hand, the controller based on the geometric mean converge slowest, which is due to the slow convergence of the heading in this case. As we increase the parameter  $m$ , the controller based on the geometric mean can converge faster. In addition, both the control inputs based on Sontag's formula and the geometric mean have chattering phenomenon compared to the SDRE and saturation controllers. This can be explained from the perspective that the desired heading rate is highly switching and discontinuous (piecewise continuous in this case) and the original Sontag's formula is designed for smooth functions and has no saturation considerations. As a comparison, saturation controller is designed with respect to the properties of the original system and accounts for the input constraints explicitly. The SDRE controller can also achieve good performance even if there is no explicit consideration for input constraints in the controller design.

Fig. 7 and 8 show the desired actual trajectories and the tracking errors respectively under large initial errors. The weighting matrices for the SDRE controller are chosen the

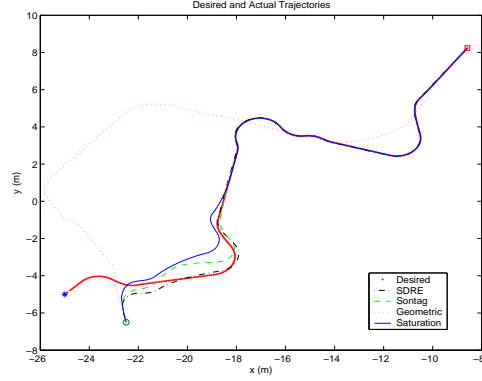


Fig. 4. The desired and actual trajectories under small initial errors.

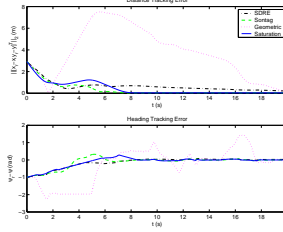


Fig. 5. The trajectory tracking errors under small initial errors.

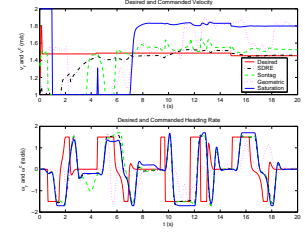


Fig. 6. The desired and actual control inputs under small initial errors.

same as the case under the small initial errors. It can be seen that the saturation controller and the controller based on the geometric mean are superior to the other two by explicitly accounting for the input constraints during the controller design procedure. In fact, the SDRE controller has the worst performance for heading tracking due to heading rate saturation.

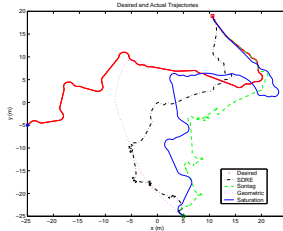


Fig. 7. The desired and actual trajectories under large initial errors.

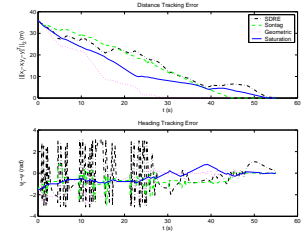


Fig. 8. The trajectory tracking errors under large initial errors.

Fig. 9 and 10 show a comparison between the SDRE controller and the saturation controller under small and large initial errors respectively. Here the weighting matrices for the SDRE controller is chosen as  $Q(x) = \text{diag}([1, 1, 1])$  and  $R(x) = \text{diag}([8, 10])$ . We can see that by properly choosing the weighting matrices  $Q(x)$  and  $R(x)$ , the SDRE controller can achieve better performance than the saturation controller under small initial errors in Fig. 9, which can be expected since the SDRE controller is proved to be locally asymptotically stable and suboptimal. However, using the same weighting matrices but under large initial errors, the SDRE controller achieves much worse performance than the

saturation controller as shown in Fig. 10 due to the input constraints.

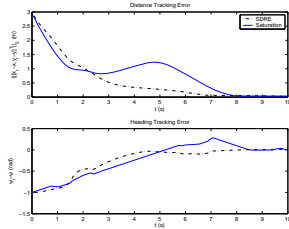


Fig. 9. The comparison between SDRE controller and saturation controller under small initial errors.

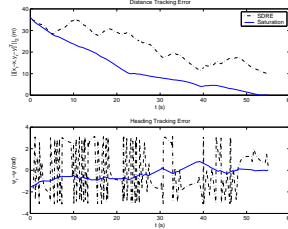


Fig. 10. The comparison between SDRE controller and saturation controller under large initial errors.

Fig. 11 and 12 show the performance of the SDRE controller without and with input constraints respectively, where  $Q(x) = \text{diag}([1, 1, 1])$  and  $R(x) = \text{diag}([0.1, 0.01])$ . We can see that the SDRE controller becomes unstable with these inappropriate weighting matrices as shown in Fig. 11. Even if good tracking performance can be achieved without input constraints in Fig. 12, huge control efforts are needed in this case.

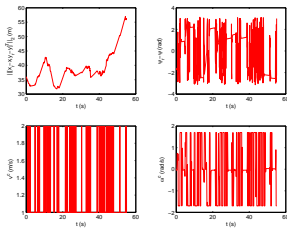


Fig. 11. The performance of SDRE controller using inappropriate weighting matrices with input constraints.

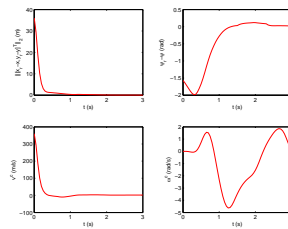


Fig. 12. The performance of SDRE controller using inappropriate weighting matrices without input constraints.

Fig. 13 shows the tracking errors of the four controllers with measurement noise. Here we assume that there is zero mean and unit variance white noise associated with the position measurement and zero mean and 15 degree variance white noise associated with the heading measurement. The weighting matrices for the SDRE controller are chosen the same as those in Fig. 9 and 10. We can see that the saturation controller has the smallest steady-state tracking errors. Under the same settings, the SDRE controller is no longer superior to the saturation controller subject to measurement noise compared to Fig. 9.

## VI. CONCLUSION

Constrained nonlinear tracking control for unmanned air vehicles is studied. Non-CLF based control approach and constrained CLF based control approaches are derived to achieve asymptotically tracking. Input uncertainties are also addressed using input-to-state stability. Detailed simulation results have shown the advantages and disadvantages of each approach under different situations.

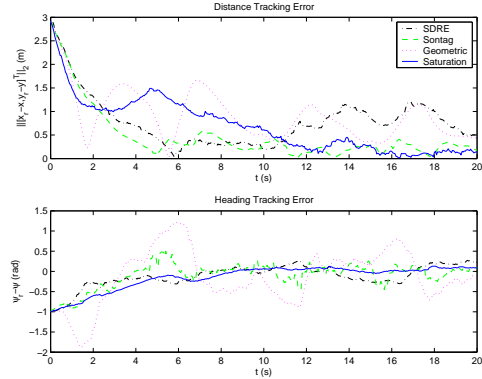


Fig. 13. The trajectory tracking errors under measurement noise.

## REFERENCES

- [1] E. D. Sontag, "A Lyapunov-like characterization of asymptotic controllability," *SIAM Journal on Control and Optimization*, vol. 21, pp. 462–471, May 1983.
- [2] Z. Artstein, "Stabilization with relaxed controls," *Nonlinear Analysis, Theory, Methods, and Applications*, vol. 7, no. 11, pp. 1163–1173, 1983.
- [3] E. F. Camacho and C. Bordons, *Model Predictive Control*. Springer Verlag, 1999.
- [4] Y. Lin and E. Sontag, "Control-Lyapunov universal formulas for restricted inputs," *Control-Theory and Advanced Technology*, vol. 10, pp. 1981–2004, December 1995.
- [5] Y. Lin and E. D. Sontag, "Universal formula for stabilization with bounded controls," *Systems and Control Letters*, vol. 16, pp. 393–397, June 1991.
- [6] W. Ren and R. W. Beard, "Clf-based tracking control for UAV kinematic models with saturation constraints," in *Proceedings of the IEEE Conference on Decision and Control*, (Maui, Hawaii), pp. 3924–3929, December 2003.
- [7] J. R. Cloutier, "State-dependent Riccati equation techniques: An overview," in *Proceedings of the American Control Conference*, pp. 932–936, 1997.
- [8] E. Sontag and Y. Wang, "New characterizations of input-to-state stability," *IEEE Transactions on Automatic Control*, vol. 41, pp. 1283–1294, September 1996.
- [9] J. W. Curtis and R. W. Beard, "Satisficing: A new approach to constructive nonlinear control," *IEEE Transactions on Automatic Control*, (to appear).
- [10] D. Kingston, R. Beard, T. McLain, M. Larsen, and W. Ren, "Autonomous vehicle technologies for small fixed wing UAVs," in *AIAA 2nd Unmanned Unlimited Systems, Technologies, and Operations—Aerospace, Land, and Sea Conference and Workshop & Exhibit*, (San Diego, CA), September 2003. Paper no. AIAA-2003-6559.
- [11] A. W. Proud, M. Pachter, and J. J. D'Azzo, "Close formation flight control," in *Proceedings of the AIAA Guidance, Navigation, and Control Conference*, (Portland, OR), pp. 1231–1246, August 1999. Paper No. AIAA-99-4207.
- [12] R. W. Beard, T. W. McLain, M. Goodrich, and E. P. Anderson, "Coordinated target assignment and intercept for unmanned air vehicles," *IEEE Transactions on Robotics and Automation*, vol. 18, no. 6, pp. 911–922, 2002.
- [13] T.-C. Lee, K.-T. Song, C.-H. Lee, and C.-C. Teng, "Tracking control of unicycle-modeled mobile robots using a saturation feedback controller," *IEEE Transactions on Control Systems Technology*, vol. 9, pp. 305–318, March 2001.
- [14] E. D. Sontag, "A 'universal' construction of Artstein's theorem on nonlinear stabilization," *System & Control Letters*, vol. 13, pp. 117–123, 1989.
- [15] M. Krstić and H. Deng, *Stabilization of Nonlinear Uncertain Systems*. Communication and Control Engineering, London: Springer, 1998.
- [16] H. K. Khalil, *Nonlinear Systems*. Upper Saddle River, NJ: Prentice Hall, 2nd ed., 1996.
- [17] W. Ren and R. W. Beard, "Trajectory tracking for unmanned air vehicles with velocity and heading rate constraints," *IEEE Transactions on Control Systems Technology*, 2003. (to appear).